



Effects of Various Heat Treatment Conditions on the AA7075 Alloy's Fatigue Behavior

Dr. Sunil Kumar K¹, Dr. Adil ahmed², Dr. S Suhael ahmed³

¹Associate Professor ,Department of Mechanical Engineering ,RLJIT,Doddaballapur,India -561203

²Associate Professor ,Department of Mechanical Engineering ,KNSIT,Bangalore ,India -64

³Assistant Professor ,Department of Mechanical Engineering ,Govt.Engg College, KR pate,India -571426

Abstract :

The impact of various heat treatment techniques applied to AA7075 alloys on the fatigue behaviour was investigated in this work. Anodizing (O), high temperature pre-precipitating (HTPP), artificial ageing (T6), retrogression, and re-aging were the procedures used on AA7075 aluminium (RRA). The samples underwent a 2-hour annealing heat treatment at 500°C before being cooled in the furnace. Following the HTPP, RRA, and T6 heat treatment operations, the samples were solution treated for two hours at e before being subjected to the artificial ageing (T6) method. The results of the fatigue testing showed that the annealed (O) samples had the lowest fatigue strength and the samples that had undergone artificial age (T6) had the maximum fatigue strength. They were heated to 500°C, cooled to ambient temperature, and then matured for 24 hours at 120°C. In the retrogression and re-aging procedure, samples were re-aged for 24 hours at 120°C after being solution treated for an hour at 220°C after the T6 method. Precipitates were created in the high temperature pre-precipitating for 30 minutes at 450°C, and then they were matured for 24 hours at 120°C. Through the use of the scanning electron microscope (SEM + EDS), hardness tests, and X-ray diffraction (XRD) techniques, all samples were analysed. At the end of experimental studies, SEM and EDS examinations XRD results revealed that η (MgZn₂) phase heat treatment procedures for T6. The results of the fatigue testing showed that the annealed (O) samples had the lowest fatigue strength and the samples that had undergone artificial age (T6) had the maximum fatigue strength.

Keywords: fatigue behaviour, various heat treatments, and AA7075 alloy

DOI Number: 10.48047/NQ.2023.21.2.NQ23054

Neuroquantology 2023; 21(2): 522-530

1Introduction

A typical application for high-strength 7xxx series aluminium alloys in the aerospace industry is due to its characteristics, such as low density and excellent strength. Studies that use various techniques to enhance these alloys' strength and other properties (such resistance to corrosion) have increased significantly in recent years [1-3]. Aging treatment is the most popular technique

used to increase strength in Al-Zn- Mg-Cu alloys. With various heat treatment procedures, the strength values of alloys in the 7xxx family can be greatly boosted [4–9]. While 7xxx series alloys gain high strength under the artificial aging (T6) conditions, they become considerably sensitive towards stress corrosion. Thus, in order to equilibrate both mechanical properties and corrosion sensitiveness under optimal con- ditions, Following the T6 heat



treatment, alloys from the 7xxx series are subjected to the retrogression and re-aging (RRA) and high temperature pre-precipitate (HTPP) ageing procedures [5, 10–12].

In the T6 heat treatment, the alloy's strength is increased by precipitates that form in the structure after the dissolution and quench operations. The following reaction [13–15] produces the precipitate that develops as saturated solid solution ages.

GP zones, saturated solid solution, and (MgZn₂) (MgZn₂). GP zones that are coherent with the matrix and spheric can be created at low temperatures because they have low interfacial energy.

2 Materials and methods

The aluminium alloy AA7075, which is frequently used in the aerospace and space industries due to its low specific weight, high strength, and electrical and thermal conductivities, was employed in the experimental experiments.

Table 1 provides the chemical make-up of the AA7075 alloy employed in the experimental studies.

The experiment-use alloy was annealed for two hours at

Zn	Mg	Cu	Fe	Cr	Si	Mn	Ti	Al
5,16	2,19	1,30	0,28	0,19	0.17	0.15	0,009	Balance

Table1:ChemicalcompositionoftheAA7075aluminumalloy

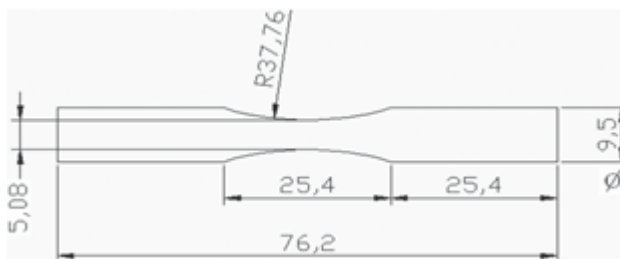


Fig.1:Dimensionsoffatiguetestsamplesusedintheexperiments

Prior to the ageing processes, the material was heated to 500°C (at a rate of 10°C/min).

The turning machine carefully handled an annealed stick of AA7075 aluminium alloy measuring 10 mm in diameter, and fatigue samples were created in accordance with the measurements shown in Figure 1 and ASTM E-606 standards.

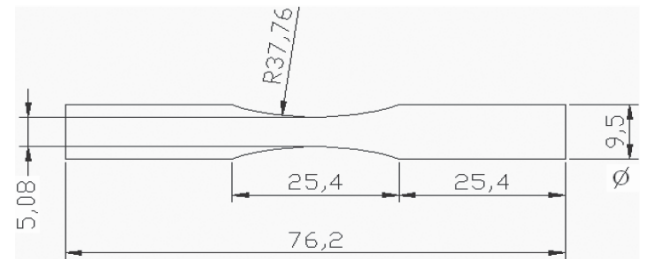
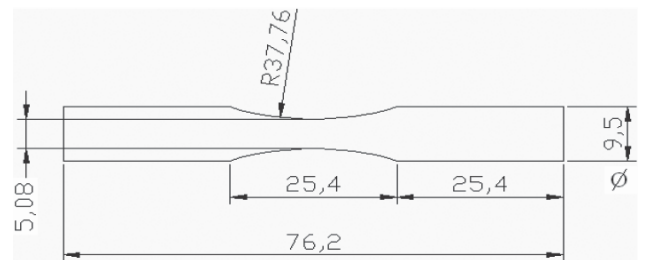
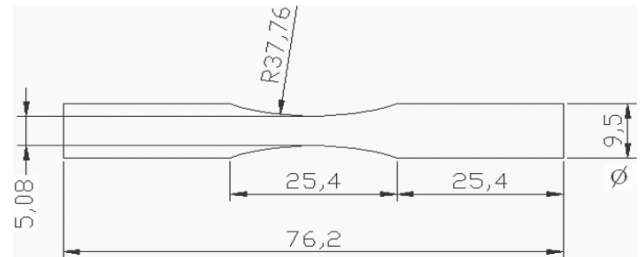
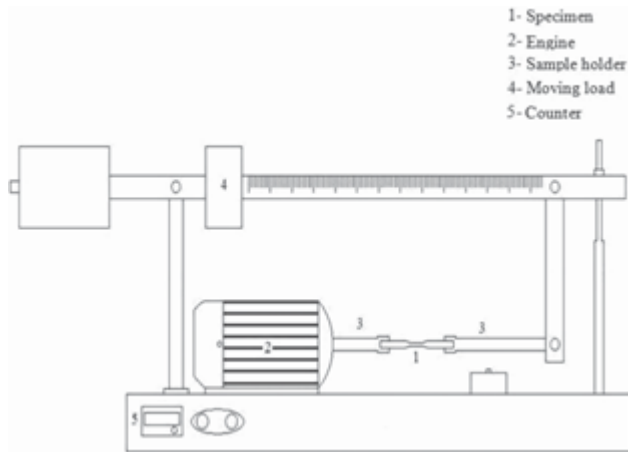
Table 2 lists the heat treatment parameters that were used in the experimental trials. As can be seen from Table 2, the prepared fatigue samples were subjected to three distinct heat treatment procedures.

The first group of samples received annealing (O), the second group of samples received T6, the third group of samples received RRA, and the fourth group of samples received HTPP heat treatment.

Heat Treatment	Solution temperature and time	Cooling	Pre-precipitating process	Ageing	Retrogression (R)	Quenching	Reaging (RA)
T6	485°C 2hours	Water 25°C	Water 25°C	120°C 24hours			
T6+RRA	485°C 2hours			120°C 24hours	220°C 1hour	25°C Saltwater	120°C 24hours
HTPP	485°C 2hours	Furnace	450°C 30minutes	120°C 24hours			
O	500°C 2hours	Furnace					



Table 2: Heat treatment parameters applied to the AA7075 aluminum alloy heat therapies for ageing. All samples were subjected to standard metallographic techniques in order to examine their microstructure. SEM and energy dispersive spectroscopy (EDS) were utilised in the characterisation experiments, while a Bruker brand X-Ray diffractometer (XRD) was used to identify the phases generated in the Al matrix at the conclusion of heat treatment. Aged samples' Brinell hardness levels were measured (HB). For each sample, five measurements were taken, and the average of these five results was determined. For the hardness tests, a ball with a diameter of 2.5 and a charge ratio of 31.25 (2.5/31.25) was employed.



524

After applying heat treatment, the surfaces of the samples being prepared for fatigue tests were lustered with 3 m diamond solution in an effort to enhance their surface quality. It was especially important to maintain this quality across all samples. The experiments were conducted using a rotary tilt test device that was created using a Wöhler type fatigue test device as a model. With this apparatus, all tests were conducted with R

(strain rate) = 1 and a 46 frequency (2780 cycles/min). The fatigue testing employed five different strain levels (200-250-300-350-400 MPa). For each load, five separate fatigue samples were examined. Tests for wear were kept going until the samples broke. After fatigue tests, samples' fractured surfaces were analysed using SEM. Wöhler type fatigue test device used in the



experiments demonstrated schematically in Figure 2.

3 Results and discussion

3.1 Microstructure examinations

Figure 3 shows SEM images of AA7075 alloy samples that have undergone various heat treatment processes and undergone annealing (O), ageing (T6), solution re-treatment and re-aging (RRA), and pre-precipitation (HTPP) at the conditions listed in Table 2.

As can be observed in Figure 3a, the process does not need the formation of precipitate phase in the microstructure of the annealed (O) sample, but because some alloy elements do not dissolve (segregate), the structure contains pores. However, secondary phase precipitates are seen as a result of ageing in the samples heated using the T6, RRA, and HTPP heat treatment methods (Figure 3b, c, and d). Additionally, when examining the grain architectures of samples that

received various heat treatments, the microstructure with the largest grains is it is also understood from SEM images

3.2 Hardness measurements

Figure 4 displays the hardness values of 7075 aluminium alloys that were annealed and aged using several heat treatment procedures (T6, RRA, and HTPP). Although the annealed samples' average hardness was found to be 68 HB, it was found that the hardness values of aged samples were nearly twice as high as those of annealed samples. Measurements of hardness confirmed that an alloy's hardness varies according to the type of ageing. While samples treated with the T6 heat treatment method had the highest hardness values (168 HB), samples treated with the RRA and HTPP heat treatment procedures showed comparable results, with 156 HB and 157 HB, respectively. The dimensional increase (growth) is blamed for this decline in hardness.

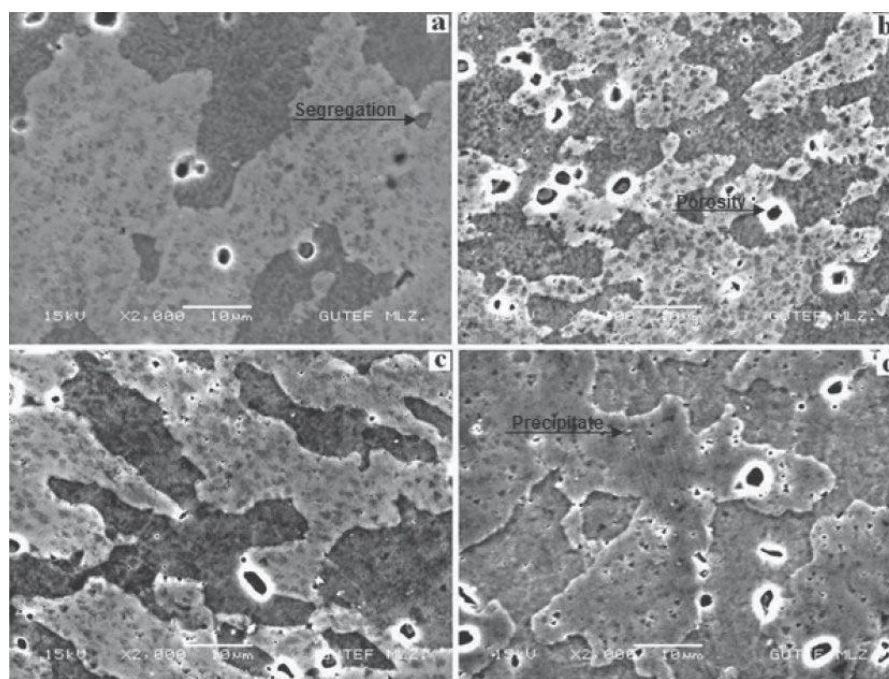


Fig.3: SEM images of the AA7075 alloy treated with different heat treatment processes O(a), T6(b), HTPP(c) and RRA(d).



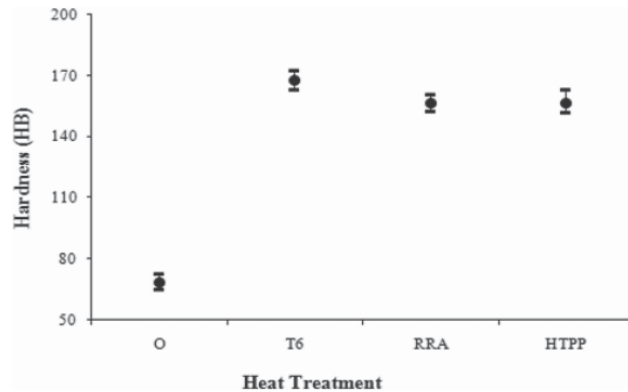


Fig.4: Hardness changes of the AA7075 alloy aged through different heat treatment processes through re-heating the samples during solution treatment, re-aging stages in RRA heat treatment following T6 procedure, as well as high temperature pre-precipitate production stage in HTPP heat treatment, precipitates) of (Mg₂Zn) precipitates that are already available in the structure. In the T6 thermal treatment, the alloy exhibits a saturated solid solution structure after being solution treated for two hours at 485°C and water quenched at room temperature. The secondary phase precipitates that are created in the matrix as a result of artificial ageing boost its strength [18]. The formation of secondary phase particles in the structure increases the material's hardness. Hardness values obtained in the present study are also in parallel to the findings of some previous studies[23,24].

3.3 XRD examinations

Results of XRD analysis obtained at $2\theta, 30^\circ \leq 2\theta \leq 90^\circ$ interval for the diffraction angle of samples treated with different heat treatments (O, T6, RRA, HTPP) are given in Figure 5. With these various ageing heat treatment procedures, secondary phase precipitates that increase strength are anticipated to occur in the alloy's structural composition. The ageing of the 7075 aluminium alloy causes some phase changes in the structure. The semi-coherent (MgZn₂) phase, which increases strength, was incoherent and stable at the conclusion of the XRD investigations, as expected (Mg₂Zn) phase and MgAl₂O₄ phase, both of which are seen in the structures of the older samples and

are assumed to occur throughout production phases. Vargas claims that MgAl₂O₄ type inclusions can also be seen in the structure in a study [25]. The structure also contained Mg_{0.971}Zn_{0.025} ve (Mg_{0.76}Zn_{0.25})O phases, which were discovered to have formed as a result of ageing heat treatment procedures but were less frequently discussed in the literature. Al and Fe are also found in the structure, among other elements. The segregations that occurred throughout the AA7075 alloy's production stages are demonstrated by the presence of Al and Fe in the structure.



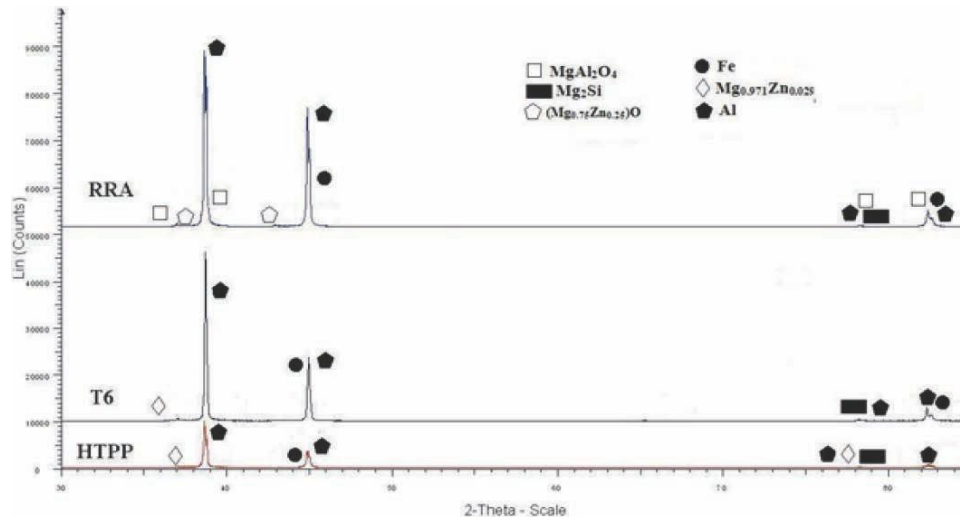


Fig.5:XRDresultsoftheaged(HTPP,T6,RRA)AA7075 alloy

A few earlier investigations have also documented the formation of additional phases in the structure throughout the ageing processes, in addition to the (MgZn₂) phase [24, 18, 19]. These phases can form precipitates within grains as well as along grain boundaries. Prior to the ageing processes, these phases that were produced during the alloy's production stages do not totally dissolve in the structure [26]. Even in trace proportions, saturated solid solutions include undissolved alloy components. It is therefore quite difficult to assert that all phases discovered through XRD analysis were created by ageing processes. However, regardless of the circumstances, the aging-related presence of these intermetallics in the structure

3.4 Fatiguetests

The strain (S) - number of cycles (N) diagram was created using the mean of the results received at the conclusion of fatigue tests. Figure 6 presents the S-N diagram that was created following fatigue tests on the AA7075 aluminium alloy that has undergone O, T6, RRA, and HTPP heat treatment treatments. based on the S - N diagram shown in Figure

527

6. It is evident from this graph that the fatigue curves of the annealed (O) samples and samples that underwent various heat treatment procedures to age them are different (T6, RRA, HTPP). This indicates that the annealed samples' fatigue strength is often lower than the samples aged under various conditions. The most severe tiredness cycle occurred in

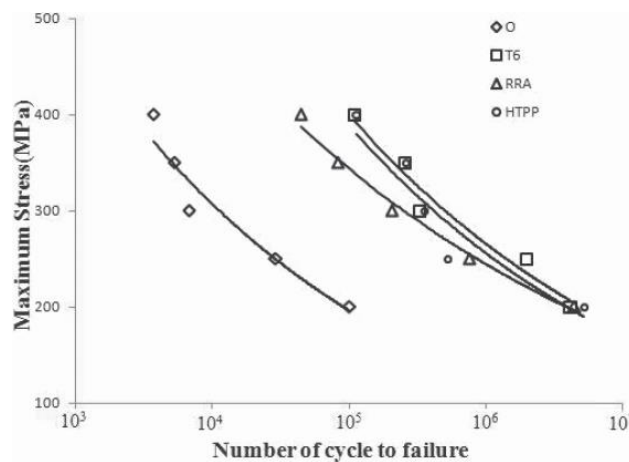


Fig.6:S–Ndiagram obtained at the end off atigue tests of the AA7075 aluminum alloy aged through O,T6,RRA and HTPP heat treatment processes

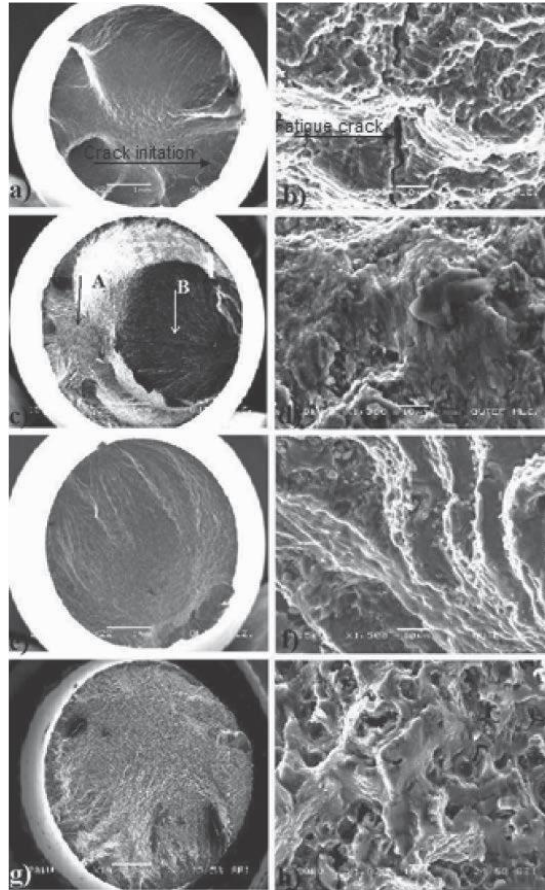


Fig.7:SEM images of broken surfaces formed at the end offatigue testsO(a,b),T6(c,d),RRA(e,f),HTPP(g,h). compared to the fatigue strength of the annealed samples, it can be noticed that the fatigue strength of the samples aged under different conditions has grown by around 40%. When the fatigue strength values of annealed samples are taken into account, it was determined that the fatigue strength has increased by roughly 106 cycles.



The fatigue strengths of the samples subjected to the HTPP and RRA procedures were quite similar. While fatigue strengths and cycle counts of materials aged by the RRA and HTPP processes are higher than those of annealed (O) samples, they are lower than those of samples aged through T6 heat treatment. The re-heating of the samples during solution treatment and re-aging stages in RRA heat treatment following T6 process as well as high temperature pre-precipitate formation stage in HTPP heat

Figure 7 shows SEM pictures of the experimental samples' fractured surfaces after fatigue testing. Figure 7c, d further shows that the sample aged after T6 heat treatment fractured in a semi-ductile manner. B-designated region, the fracture zone). It is understood that, when compared to samples aged with T6 heat treatment, the fracturing of samples aged by RRA (Figure 7e, f) and HTPP (Figure 7g, h) heat treatment has a more ductile fracturing mode. Large cavities that have developed on the sample's surface indicate ductile fracturing. After a given number of cycles, the microcracks that occur on the sample surface as a result of the load and cycle count during the fatigue tests move towards the centre, merge, and expand into macrocracks, which induce breaking. On the damaged surfaces, fatigue fractures, inclusions, and second phase particles generated in the structure over time are visible. Generally, inclusions happen 10 metres below the surface. They underline that these inclusions or regions near them are where microcracks that form during fatigue originate in a study on the same alloy by Shadzaad et al. [27]. Examining the cracked surfaces shown in Figure 6 makes it clear that microcracks originate from regions with inclusions, coarse second-ary phase

treatment is responsible for these changes in the fatigue strengths of the material. This dimensional increase (growth of precipitates) of (Mg₂Zn) precipitates that are already present in the structure is also responsible. Taking into account the cycle's fatigue resistance for 105 cycles, it38% of samples that underwent the RRA procedure. On the other hand, samples heated using the HTPP procedure showed fatigue strength values that were comparable to those of samples heated using the T6 method.

particles, and microstructural flaws. Additionally, the structure contains some alloy components that did not completely dissolve during the solution treatment. Microcracks that form during fatigue tests form mostly between the alloy elements that were discovered undissolved.

4 Conclusion

This study can be used to infer the following conclusions from the experimental studies:

1. It was discovered that the hardness of the samples subjected to the various heat treatment processes (O, T6, RRA, HTPP) varied depending on the technique used. The samples that underwent T6 heat treatment had the highest measured hardness value; samples that underwent HTPP and RRA procedures had the next-highest recorded hardness values.
2. XRD analyses confirmed that secondary phase (Mg₂Zn) precipitates were created by age, which was expected. Additionally, Mg_{0.971}Zn_{0.025} ve (Mg_{0.76}Zn_{0.25})O phases that had not received much attention in the literature up until that point were found.
3. It was discovered that the heat treatment applied to the sample after the fatigue testing affected the fatigue strength. The samples treated with the artificial ageing (T6) technique showed the maximum fatigue strength, while



the samples that had been annealed showed the lowest fatigue strength.

REFERENCES:

1. Giménez, S.; Vleugels, J.; Vander Biest, O. In situ investigation of dewaxing and sintering of stainless-steel powder compacts by impulse excitation. *Scr. Mater.* 2008, 58, 985–988. [CrossRef]
2. Heinz, S.; Eifler, D. Crack initiation mechanisms of Ti6Al4V in the very high cycle fatigue regime. *Int. J. Fatigue* 2016, 93, 301–308. [CrossRef]
3. Hansen, N. The effect of grain size and strain on the tensile flow stress of aluminium at room temperature. *Acta Metall.* 1977, 25, 863–869. [CrossRef]
4. Hansen, N. Hall–Petch relation and boundary strengthening. *Scr. Mater.* 2004, 51, 801–806. [CrossRef]
5. Kouzeli, M.; Mortensen, A. Size dependent strengthening in particle reinforced aluminium. *Acta Mater.* 2002, 50, 39–51. [CrossRef]
6. Yonenaga, I.; Motoki, K. Yield strength and dislocation mobility in plastically deformed bulk single-crystal GaN. *J. Appl. Phys.* 2001, 90, 6539–6541. [CrossRef]
7. Fleischer, R. L. Rapid solution hardening, dislocation mobility, and the flow stress of crystals. *J. Appl. Phys.* 1962, 33, 3504–3508. [CrossRef]
8. Chai, G.; Zhou, N. Study of crack initiation or damage in very high cycle fatigue using ultrasonic fatigue test and microstructure analysis. *Ultrasonics* 2013, 53, 1406–1411. [CrossRef][PubMed]
9. Zuo, J. H.; Wang, Z. G.; Han, E. H. Effect of microstructure on ultra-high cycle fatigue behavior of Ti–6Al–4V. *Mater. Sci. Eng. A* 2008, 473, 147–152. [CrossRef]
10. Ahn, D. G.; Amanov, A.; Cho, I. S.; Shin, K. S.; Pyoun, Y. S.; Lee, C. S.; Park, I. G. Gigacycle fatigue behavior by ultrasonic nano crystalline surface modification. *J. Nanosci. Nanotechnol.* 2012, 12, 5902–5906. [CrossRef][PubMed] © 2018

